Volume 16, Issue 4, 162530 (1-13)

International Journal of Nano Dimension (IJND)

https://dx.doi.org/10.57647/j.ijnd.2025.1604.30

Evaluation of the catalytic and *in-vitro* anticancer potential of Gold nanoparticles synthesized using clammy cherry (*Cordia Obliqua Willd*)

Anjaly Mathew[1], Aswathy Jayaprakash[2], Aneetha Mundakassery Ratnamma[2], Sandhya Paleri Veetil[2], Zeena Pallimittath Hamza[2], Amrutha Sivarajan[2], Rejimon Pooppanathara Kochappan[2], Ramla Kudukkil Thahathuveettil[3], Jasmin Jose[4], Kavitha Jacob[5], Femina Kanjirathamthadathil Saidu[2,*]

[1]*Department of Chemistry, Sree Neelakanta Government Sanskrit College, Pattambi, Kerala, India.*
[2]*Department of Chemistry, Maharaja's College Ernakulum, Kerala, India.*
[3]*Department of Physics, PTM Government College Perinthalmanna, Malappuram, Kerala, India.*
[4]*Department of Basic Science and Humanities, Jyothi Engineering College Cheruthuruthy, Thrissur, Kerala, India.*
[5]*Department of Chemistry, Bishop Abraham Memorial College, Thuruthicadu, Pathanamthitta, Kerala, India.*

[*]**Corresponding author:** femina@maharajas.ac.in

Original Research

Received:
20 January 2025
Revised:
14 April 2025
Accepted:
5 May 2025
Published online:
10 May 2025
Published in issue:
17 May 2025

Abstract:

The synthesis of metal nanoparticles using environmentally friendly materials like fruit extracts offers the benefits of eco-friendliness and compatibility for pharmaceutical and other biomedical applications. The phytogenic synthesis can be conducted at convenient ease under microwave exposure. Here, through a microwave-assisted, fast, and cost-effective approach, monodispersed, spherical gold nanoparticles (AuNPs) with outstanding catalytic efficiency and anticancer activity were successfully synthesized using the extract of clammy cherry (*Cordia Obliqua Willd*) fruit. UV-Visible spectroscopic analysis, SEM, and HRTEM analysis have been used to characterize the prepared AuNPs. The electronic spectrum investigations have revealed that the MW power, length of exposure, gold ion concentration, and content of the cherry extract had a substantial impact on the rate of production, size, and surface plasmon absorption of AuNPs. According to TEM examinations, AuNPs are crystalline and spherical in shape, with a mean size of 11.7 nm. Anticancer activity of the stabilized AuNPs studied against Dalton's lymphoma Ascites cells confirmed that the stabilized AuNPs were highly effective for the apoptosis of cancer cells selectively. Furthermore, the AuNPs' catalytic efficiency in reducing hazardous organic pollutants viz. methyl orange (MO), methylene blue (MB), and methyl red (MR), 2-nitrophenol (2-NP) and 4-nitrophenol (4-NP), with borohydride-aided reduction proved appealing for environmental pollution remediation applications.

Keywords: Anticancer activity; Catalysis; Green synthesis; Gold nanoparticles; Methyl orange; Microwave; Reduction; Nitrophenol

1. Introduction

The production of metal nanoparticles (MNPs) and composites have sparked a lot of interest recently owing to their extraordinary physio-chemical properties and a wide variety of biological, sensing, and catalytic applications [1–8]. When compared to other MNPs, gold nanoparticles (AuNPs) have been widely investigated owing to their low toxicity to microorganisms and mammalian cells. Many researchers have reported excellent anticancer, antioxidant and antibacterial activity of stabilized AuNPs [9–19]. Biosensors for virus, bacteria, and pathogen detection, as well as biomedical research applications such as nano bio diagnostics and controlled drug administration, use AuNPs extensively [20, 21]. Surface-enhanced Raman spectroscopy, optical sensors, and biological applications have all been described to use AuNPs earlier. Using $NaBH_4$, biosynthesized AuNPs were used to catalyze the reduction of different nitro compounds. Gold nanocatalysts were used as a highly selective colorimetric nanoprobe for many metals like Cd^{2+}, Pb^{2+},

Ni^{2+}, Hg^{2+} etc. [22–27]. Degradation of carcinogenic organic compounds like dyes and aromatic compounds were also performed using AuNPs [28–31].

Because of the enormous amount of capital involved in manufacturing and the energy intensive process, the biological technique of synthesis of nanoparticles (NPs) has proven to be a better way than chemical methods. Since toxic chemicals like hydrazine are used, the approach is not environmentally friendly [31, 32]. These shortcomings pushed for a "greener synthesis of NPs" that is both ecologically friendly and enable greater control of crystal formation, stabilization and size. As a bottom-up synthetic strategy, plant and fungal extract-mediated solution phase synthesis of AuNPs via Au (III) reduction to Au (0) has recently gained attraction. Its advantages include green reducing and stabilizing chemicals, an environmentally friendly aqueous medium, and mild reaction conditions. Phytochemicals extracted from various parts including leaf, bark, root, fruit and stem of number of plants have all been used in the biogenesis of AuNPs [33–37]. However, when compared to conventional chemical reduction, phytochemical reduction procedures for the manufacture of AuNPs are significantly slower. To address this disadvantage, plant-mediated synthesis must be combined with microwave (MW) assisted synthesis. An increase in reaction rate, mild reaction conditions, higher yield of the products, low consumption of energy are certain benefits of MW heating over conventional ovens and many successful reports on MW assisted synthesis of AuNPs are available recently [38–42].

With this background, we wished to reveal the synthesis of AuNPs through a quick MW assisted green reduction of Au (III) ions from chloroauric acid. The study examined the ability of phytochemicals in clammy cherry (*Cordia Obliqua Willd*) extract as an environmentally friendly reducing and stabilizing agent for AuNPs synthesis [43–45]. Clammy cherry is a plant that belongs to Boraginaceous family which has widely distributed warmer regions of India and Ceylon. The herb has long been thought to have medicinal properties. According to traditional system, it possesses anthelmintic, purgative, diuretic, expectorant, antipyretic, hepatoprotective and analgesic action. Evaluation of pharmacological activities confirmed. *Cordia Obliqua Willd* plant has as antimicrobial, hypotensive, respiratory stimulant, diuretic and anti-inflammatory drug. Phytochemical screening revealed several polyfunctional components such as carbohydrates, flavonoids, phenolic compounds, proteins, alkaloids, amino acids, and glycosides in clammy cherry extracts. The ability of phytochemicals present in the aqueous extract of clammy cherry to reduce and stabilize metal nanoparticles has been demonstrated in our earlier work [46]. It was also planned to study the effect of MW power, time of irradiation, and composition of the reaction mixture on AuNPs properties. The study also aims to evaluate the anticancer activity of the produced AuNPs against Dalton's lymphoma ascites (DLA) cells. Moreover, the reduction of harmful water pollutants such as methyl orange (MO), methylene blue (MB), and methyl red (MR), as well as 2-nitrophenol (2-NP) and 4-nitrophenol (4-NP), were used to test the catalytic activity of biosynthesized AuNPs to establish their environmental remediation applications. This work has been reported for the first time, the clammy cherry mediated synthesis of AuNPs, anticancer, and catalytic efficacy.

2. Experimental

2.1 Materials and methods

Merck Chemicals Ltd, Mumbai, India, provided the chloroauric acid ($HAuCl_4$) and sodium borohydride ($NaBH_4$) utilized in the study. Nice Chemicals, India, provided methyl orange, methylene blue, methyl red, 4-nitrophenol and 2-nitrophenol. The AuNPs were synthesized in a domestic microwave oven.

2.2 Preparation of clammy cherry fruit extract

Clammy cherry fruits were collected from Ernakulam district (Lat 9.970715°, Long 76.281774°), Kerala State, India and were later authenticated [46]. To remove the dust, the fruits were first carefully cleaned with tap water and then with distilled water. The fruits were allowed to dry naturally in the air at room temperature. 5 g of clammy cherry fruit was cut into small pieces and mixed with 200 mL of distilled water before being microwaved for 3 minutes to extract the biomolecules found in the fruit. In hot conditions, the fruit extract was filtered through Whatman No.1 filter paper to remove fibrous impurities. The filtrate was collected and stored in refrigerator for further studies.

2.3 Microwave assisted synthesis of gold nanoparticles

For getting AuNPs, 10 mL of clammy cherry extract (10 g/100 mL) and 20 mL of 0.05 mM $HAuCl_4$ solution were mixed and irradiated in a MW oven at 2.45 GHz under 420 W. The solution turned pink, showing the formation of AuNPs. The influence of synthesis parameters like MW power, exposure time, and the composition of $HAuCl_4$ to clammy cherry extract were also studied. The whole processes were analyzed by recording the UV-Vis spectra of the reaction mixture at definite time periods.

2.4 Characterization

The UV-Vis spectral studies were performed with scientific evolution 160 UV-Visible spectrometer. The VEGA3 TESCAN scanning electron microscope (SEM) was used to study surface morphology of AuNPs. Field Emission Scanning Electron Microscopic images of the synthesised AuNPs were taken in a Carl Zeiss Sigma TM Series microscope. Transmission electron microscopic images were collected using a JEOL JEM-2100 microscope. Perkin Elmer FTIR spectrometer was used to record FTIR spectra of the vacuum dried clammy cherry extract in the range $4000 - 450\ cm^{-1}$.

2.5 Cytotoxicity of AuNPs in DLA cells

The biosynthesized AuNPs was studied for short term *in vitro* cytotoxicity using Dalton's lymphoma Ascites cells. The tumor cells aspirated from the peritoneal cavity of tumor bearing mouse was washed thrice with phosphate buffered cell line or normal cell line. The cell viability was determined by trypan blue exclusion method. A viable cell

suspension (1×10^6 cells in 0.1 mL) was introduced to tubes holding varying concentrations of AuNPs. The volume was made up to 1 mL by means of phosphate buffered cell line. The cell suspension alone was taken a control tube and these assay mixtures were incubated at 37 °C for 3 hours. The cell suspension was mixed with 0.1 mL of 0.1% trypan blue for 2-3 minutes and before being put into a hemocytometer. Dead cells absorb the blue colour of trypan blue, while the living cells do not. The numbers of stained and unstained cells were individually counted.

$$\% \text{ of toxicity} = \frac{\text{No.of dead cells}}{\text{No.of live cells+No.of dead cells}} \times 100$$

2.6 Catalytic activity studies

The catalytic activity of the prepared AuNPs towards the reduction of organic substrates including MO, MB, MR, 4-NP or 2-NP with a relatively higher concentration of $NaBH_4$ was determined. In a typical catalytic reaction, 2 mL of dye solution (10 mg/L) and 0.05 mL of AuNPs colloid were mixed with 0.5 mL of 0.05 M $NaBH_4$ solution. UV-Visible spectra of the reaction mixture were taken regularly to monitor the progress of catalytic process.

3. Results and discussion

3.1 Synthesis of AuNPs and UV-Vis spectral studies

Here, the excellent reducing and stabilizing potential of the various poly-functional molecules present in the clammy cherry were utilized for the synthesis of extremely stable AuNPs [44, 46]. The visible colour change of the solution from colorless to pink within a short time indicated the fast formation of AuNPs. The use of MW energy has significantly shortened reaction time and boosted AuNPs yield throughout the current procedure. Figure 1 shows the schematic representation of the biosynthesis of AuNPs.
As the extent of MW exposure upon reaction mixture progresses, the color got intensified as shown in Fig. 2.
In the UV-Vis spectrum of the $HAuCl_4$ solution and clammy cherry extract no absorption peaks were seen in the visible region, while absorption peaks at 301 nm and 283 nm were observed for $HAuCl_4$ solution and clammy cherry extract solution respectively in the UV-region. However, the spectra of the microwave exposed mixture of clammy cherry extract were and Au^{3+} solution have a typical surface plasmon resonance absorption band with λ_{max} around $527 - 541$ nm (Fig. 3 (a)) in the visible region. This observation confirmed the formation of AuNPs having a size less than 20 nm [47–49].

Figure 1. Pictorial illustration of MW-assisted synthesis of AuNPs using clammy cherry extract.

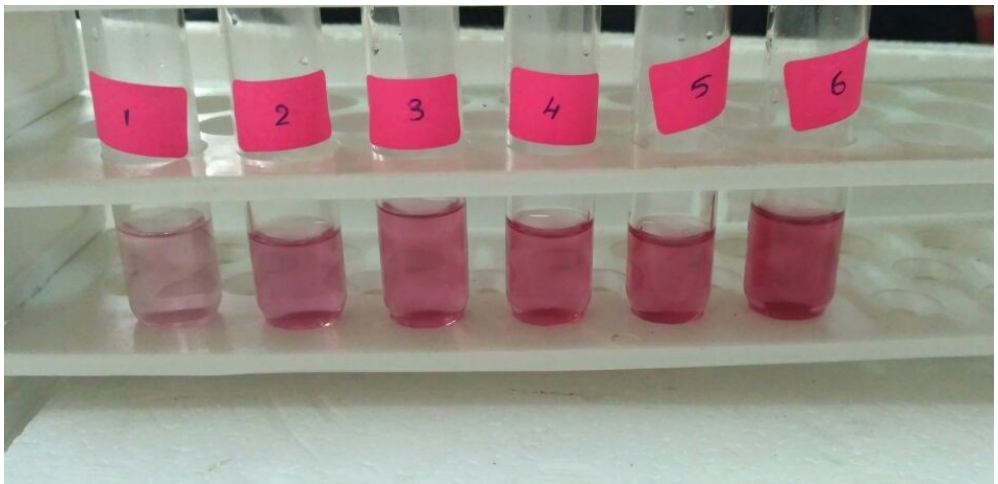

Figure 2. Color change during MW exposure of $HAuCl_4$ with clammy cherry extract.

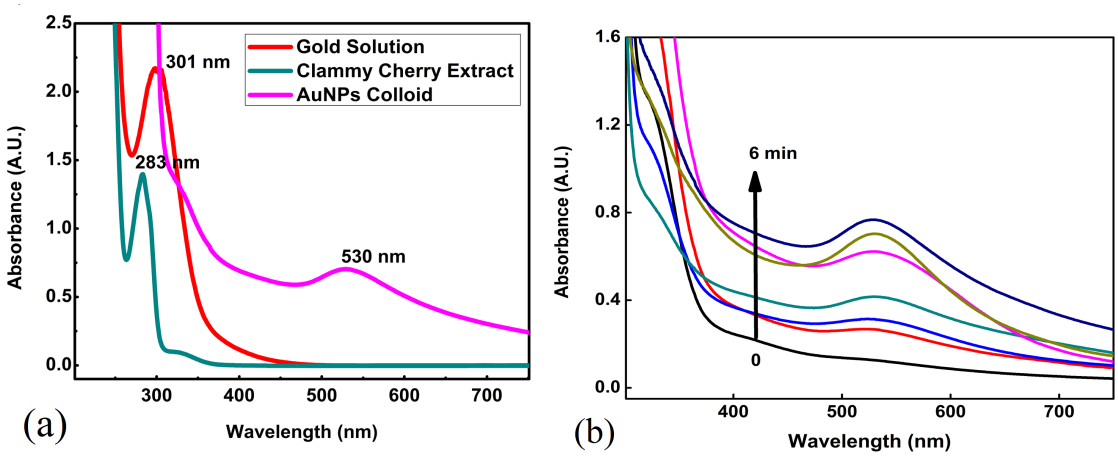

Figure 3. (a) UV visible spectra of Clammy cherry extract (green), $HAuCl_4$ solution (red), and AuNPs solution after a month (pink), (b) UV-Visible spectra recorded at different time intervals.

The stability of prepared AuNPs is considered as an important parameter and good stability recommended for catalytic, sensing and biomedical applications. It was observed that prepared AuNPs remained in colloidal form even after a month from its preparation which confirmed that interaction of clammy cherry derived phytochemicals has stabilized AuNPs effectively.

The rate of formation, size, and optical properties of AuNPs are found to be influenced by the composition of extract, MW power level and time of exposure. The $HAuCl_4$ solution and clammy cherry extract were taken in ratio of 1:4 by volume, exposed to MW radiation at power level of 420 W and UV-Visible spectrum of the mixture recorded at an interval of 1 minute is presented in Fig. 3 (b). The spectral studies suggested that duration of exposure had a influenced the amount and nature of AuNPs formed. As the extent of exposure increases, an increase in the SPR absorption intensity was observed which indicated the formation of more AuNPs due to further reduction. Furthermore, as time prolapse, a red shift in SPR maxima from 536 to 527 nm was also observed. After 6 minutes of MW exposure the intensity of absorption remained almost same confirming that reduction of Au^{3+} ions were almost complete.

The effect of MW power level on nature and distribution of AuNPs was studied by analysing the UV-Vis spectra recorded with AuNPs colloid obtained at different power while keeping the composition and period of exposure constant. At lower MW power the colour intensity was less, while the reaction mixture becomes more intensely colored as the MW power was increased which might be due to the faster reduction at higher MW power (Figs. 4 (a), 4 (b)). No significant change was observed in the case of SPR absorption maxima, while the curve becomes much sharper as the power increases indicating that narrow size distribution of AuNPs that might be due to the faster formation of stabilized AuNPs.

Keeping the MW power level at 420 W and time of MW exposure (5 min) constant, the composition of reaction mixtures taken were varied as per the Table 1 and UV-Vis spectra were recorded in each case and presented in the Fig. 5. The study revealed that even at lower proportion of extract, Au^{3+} ions are effectively reduced and resulted AuNPs were well stabilized. A direct dependenece between the intensity of SPR absorption and hence population of AuNPs with

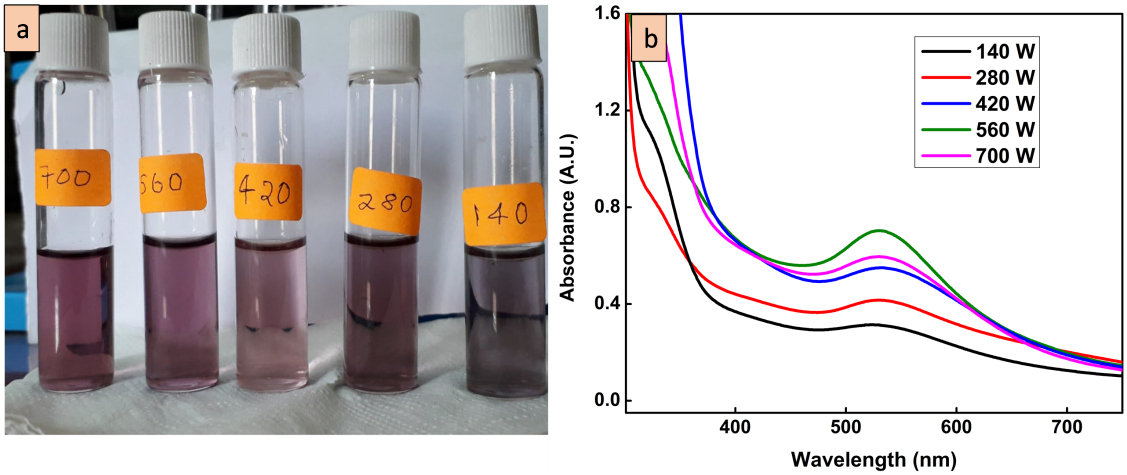

Figure 4. (a) Color change observed after MW exposure of $HAuCl_4$ (0.05 mM) and clammy cherry extract (10 g/L) for 5 minutes under different power level and (b) UV-Visible spectra recorded at different MW power.

Table 1. Synthesis conditions and corresponding λ_{max} values of AuNPs.

Volume of [$HAuCl_4$] (0.05 mM)	Volume of extract (0.1 g/mL)	MW power (W)	Time of exposure (min)	SPR λ_{max} (nm)∓1
20	5	140	5	530
20	5	280	5	530
20	5	420	5	530
20	5	560	5	531
20	5	700	5	533
20	5	420	1	536
20	5	420	2	538
20	5	420	3	534
20	5	420	4	531
20	5	420	5	530
20	5	420	6	526
5	5	420	5	541
10	5	420	5	537
15	5	420	5	533
20	5	420	5	530

the propotion of chloroauric acid solution was observed. At higher Au^{3+} concentration, the intensity of absorption increased and UV-Vis spectra observed became sharper indicating narrow AuNPs size distribution. The spectra with single SPR absorption maxima also indicated that the synthesised AuNPs were spherical. Accordingly, optical studies established the unique capping/passivating potential of the clammy cherry extract for the AuNPs synthesis. Table 1 summarizes the details of synthesis condition and corresponding SPR absorption maxima of AuNPs.

3.2 FTIR studies

FT-IR spectral studies of the vacuum-dried clammy cherry extract and AuNPs were carried out and are presented in Figure 6. The broad peak at 3398 cm^{-1} of the fruit extract is due to stretching vibrations of the phenolic O-H group that is hydrogen bonded. The peak at 2926 cm^{-1} corresponds to C-H stretching vibrations. The medium band at 1637 cm^{-1} corresponds to the amide I band. The peak around 1323 cm^{-1} is assigned to the –COO stretching from amino acid groups. The peak at 794 cm^{-1} is due to=C-H stretching (aromatic). Hence, it is concluded that these identified functional groups is responsible for the reduction of Au^{3+} ion to Au^0 and interact via coordination to yield stable AuNPs. Furthermore they might have interacted with AuNPs and prevented their clustering by forming a capping layer over the AuNPs, thus offered proper stabilization [29]. The small change in the intensity and position of the peaks in the spectrum of AuNPs can be attributed to the coordination of phytochemicals with the metals.

3.3 SEM analysis

Fig. 7 (a) shows the scanning microscopic images of synthesized AuNPs. It was found that the clustered AuNPs forms well-defined spherical microstructures. SEM studies revealed that AuNPs are effectively passivated and evenly

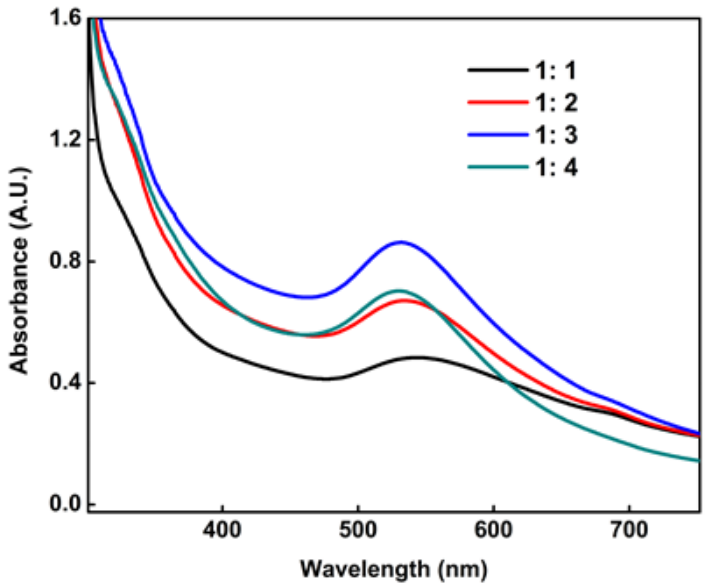

Figure 5. UV-Vis spectra of AuNPs prepared by taking different clammy cherry extract to $HAuCl_4$ solution volume ratio.

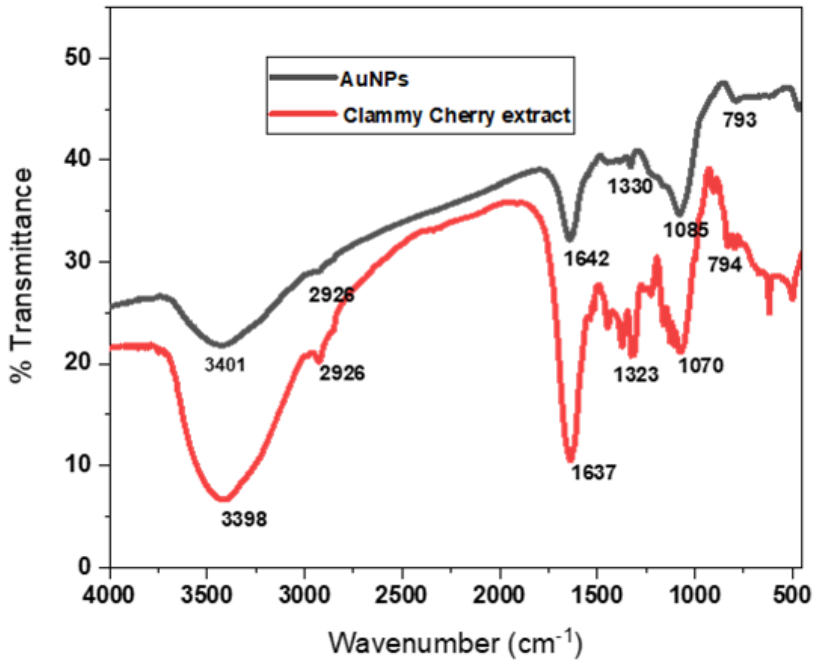

Figure 6. FTIR spectra of Clammy cherry fruit extract and AuNPs.

distributed. FESEM image of AuNPs shown in the Fig. 7 (b) further confirms that gold nanoparticles are uniformly dispersed in the phytochemical matrix.

3.4 HRTEM analysis

HRTEM studies were used to study the surface features of the biosynthesized AuNPs in greater detail (Figs. 8 a-c). The TEM studies confirmed that synthesized AuNPs were spherical. The tiny size and narrow size distribution are attributable to the rapid reduction and improved stabilization of AuNPs by the cherry-derived phytochemicals under MW irradiation. The concentric ring in the selected area electron diffraction (SAED) pattern shows the crystalline nature of AuNPs (Fig. 8 c). From the particle size distribution histogram (Fig. 8 d), the average particle size is found to be 11.7 nm. The AuNPs are effectively dispersed from one another, and no particle aggregation was found, supporting the efficient capping ability of clammy cherry derived phytochemicals.

3.5 Catalytic studies

The reductive degradation of selected organic pollutants including MB, MO, MR, 4-NP, and 2-NP with excess of $NaBH_4$ as reductant, was studied to evaluate the catalytic activity of biosynthesized AuNPs. When the mixture of dye solution and borohydride was kept free of AuNPs, no noticeable colour change was detected. Upon adding AuNPs to the above solution, the intensity of the solution's colour decreased significantly faster, indicating that the degradation was accelerated. As the reaction progressed, the solution eventually became colorless indicating that the reduction was complete. The progress of the reaction was monitored

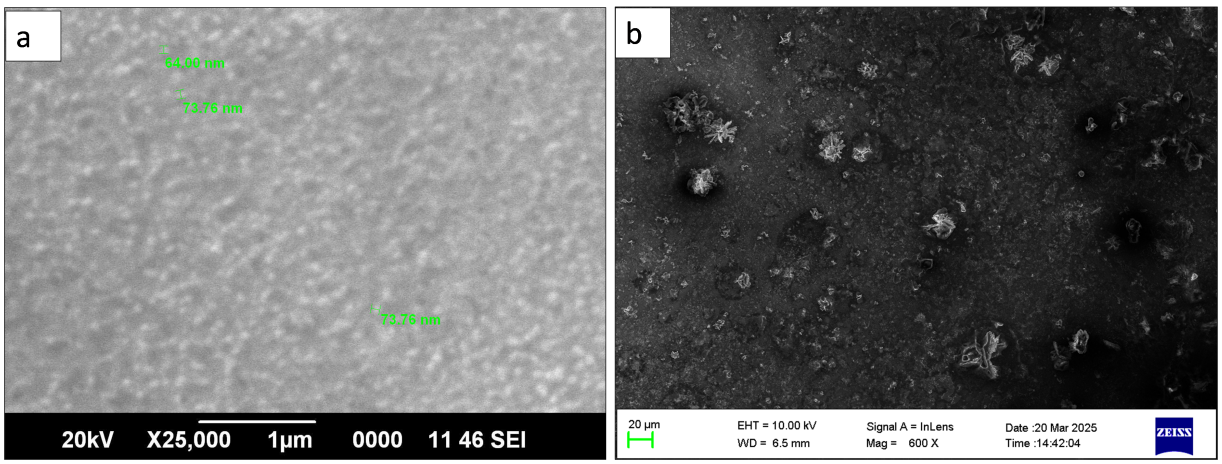

Figure 7. SEM image of AuNPs (a), FESEM image of AuNPs (b).

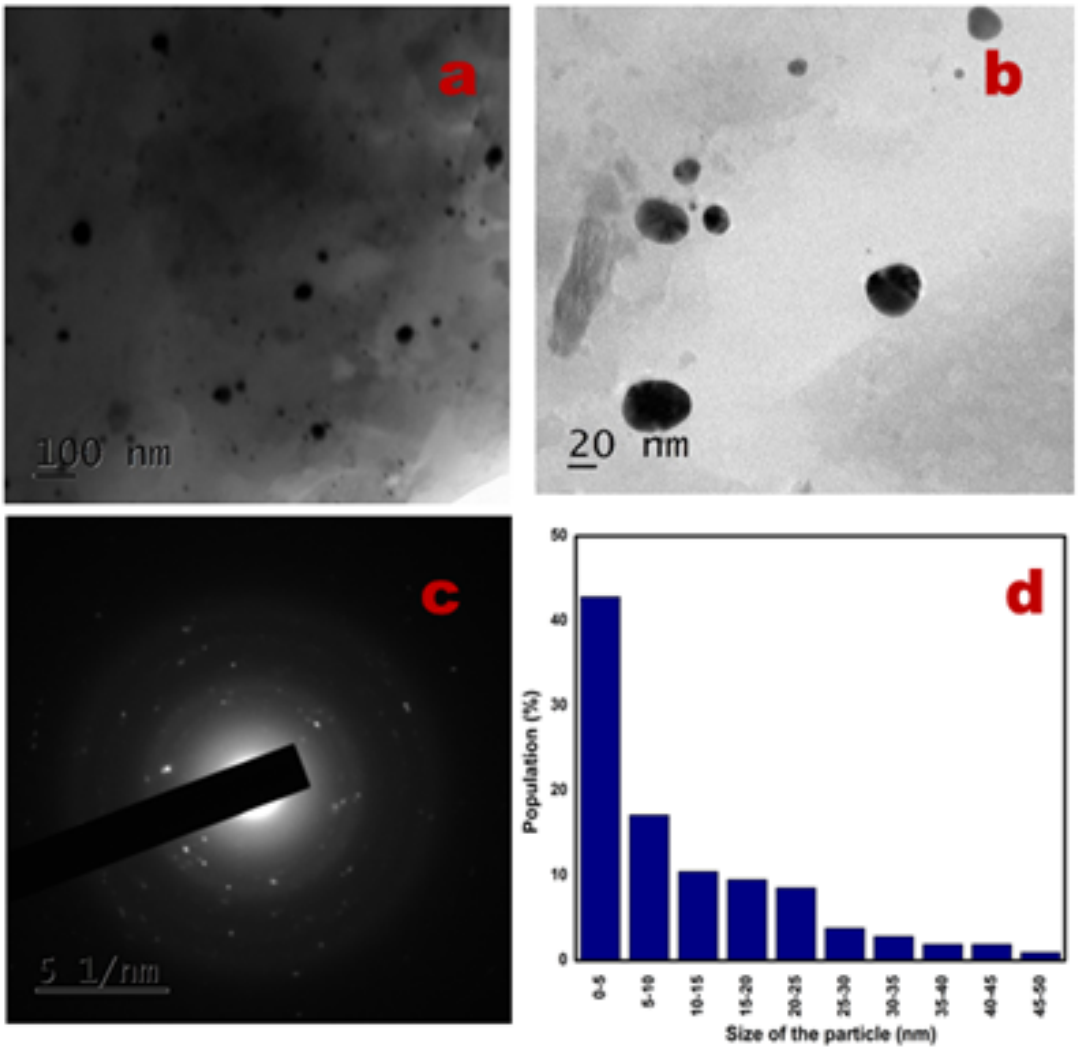

Figure 8. TEM of AuNPs under different magnification (a and b), SAED pattern (c) and Particle –size histogram (d).

by UV-Visible spectroscopy. The pseudo first order rate constant (k) for each reaction was determined from the slope of the plot of $\ln(A/A_0)$ against time (t), where A is the absorbance at λ_{max} for each substrate at a time and A_0 is absorbance at $t = 0$.

The time-dependent UV-Vis spectra for MB reduction and plot ln (A/A_0) against time are presented in Figs. 9 (a), 9 (b), respectively. For MB the absorption maximum (λ_{max}) was at 664 nm. The spectral studies showed that the reduction of MB to colorless leuco MB was fast in presence of catalyst and completed within 8 minutes. The pseudo first order rate constant k_{MB} observed was 0.5014 min^{-1}.

Figs. 10 (a), 10 (b) display the time-dependent UV-Vis spectra for MO reduction and plot ln (A/A_0) against time. For

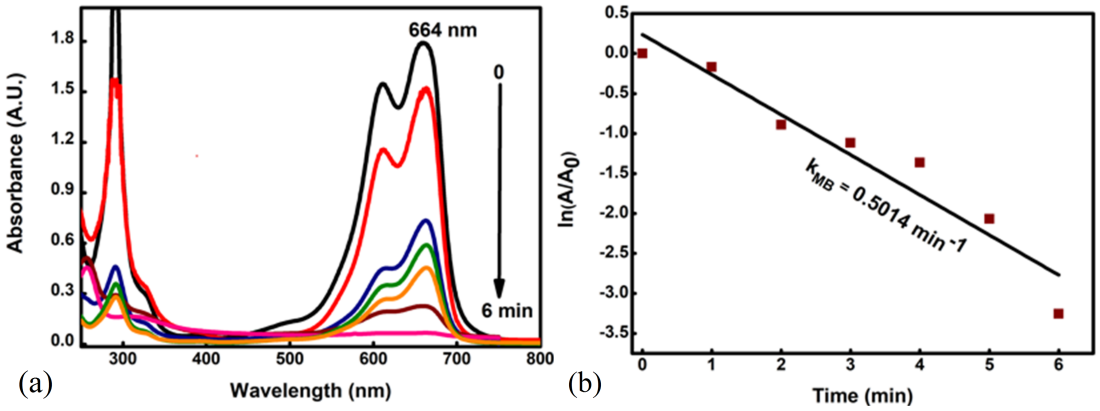

Figure 9. Time dependent UV-Visible absorption spectra for the AuNPs catalyzed reduction of MB (a) and plot of ln (A/A_0) against time (b).

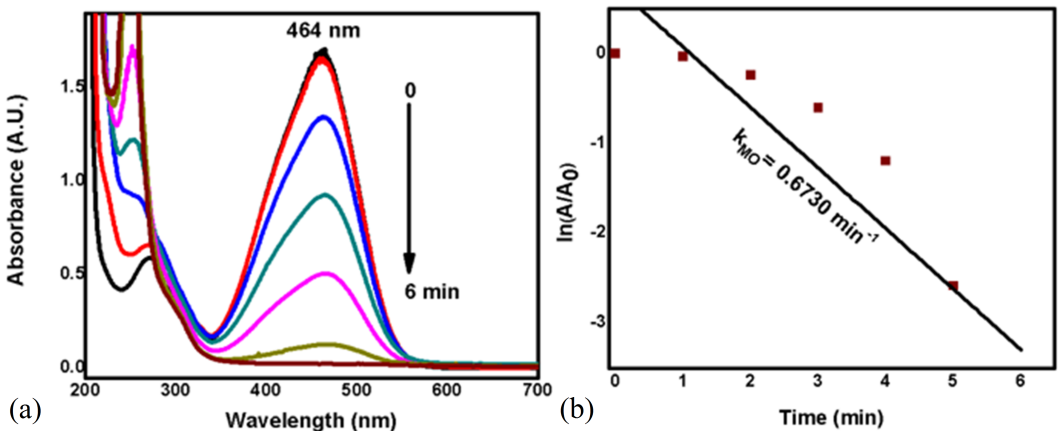

Figure 10. UV-Visible absorption spectra for the AuNPs catalyzed reduction of MO (a) and plot of ln (A/A_0) against time (b).

MO the absorption maximum (λ_{max}) was at 430 nm. The spectral studies showed that the reduction of MO to colorless reduced products was fast in presence of catalyst and completed within 8 minutes. The pseudo first order rate constant k_{MO} observed was 0.6730 min^{-1}.

The time-dependent UV-Vis spectra for catalyzed MR reduction and plot ln (A/A_0) against time are presented in Figs. 11 (a), 11 (b) respectively. The spectra of MR show the absorption maximum (λ_{max}) at 464 nm. The spectral studies showed that the reduction of MR to colorless reduced products was fast in presence of catalyst and completed within 8 minutes. The pseudo first order rate constant k_{MR} observed was 0.2744 min^{-1}.

The time-dependent UV-Vis spectra for catalyzed 4-NP reduction and plot ln (A/A_0) against time are presented in Figs. 12 (a), 12 (b) respectively. For 4-NP the absorption maximum (λ_{max}) was at 317 nm in neutral medium and upon adding $NaBH_4$ the medium became alkaline and 4-NP dissociates to yield intensely colored 4-nitrophenolate ion with λ_{max} at 400 nm. As the reaction progresses 4-NP is reduced to colorless 4-aminophenol (4-AP) which has less intense absorption at λ_{max} 300 nm. The spectral studies showed that the reduction of 4-NP to 4-AP was fast in presence of AuNPs and completed within 14 minutes. The pseudo first order rate constant $k_{4\text{-NP}}$ observed was 0.1898 min^{-1}.

The time-dependent UV-Vis spectra for 2-NP reduction and plot ln (A/A_0) against time are presented in Figs. 13 (a), 13 (b) respectively. 2-Nitrophenolate ion has absorption maximum (λ_{max}) at 418 nm and the reduced product 2-aminophenol has maximum absorption (λ_{max}) at 288 nm. As the reaction progresses 2-NP is reduced to colorless 2-aminophenol (2-AP) which has less intense absorption at (λ_{max}) 288 nm. Compared to 4-NP reduction, the spectral studies showed that the reduction of 2-NP to 2-AP in presence of AuNPs was faster and completed within 9 minutes. The pseudo first order rate constant k_{2-NP} observed was 0.2169 min^{-1}.

Earlier literature suggested that the reductive degradation of organic dyes catalyzed by MNPs involves a rapid electron transfer from the donor borohydride to the acceptor dye molecules [59, 60] The reductant BH^{4-} and dye molecules may become adsorbed on the surface of AuNPs without interfering with their action. The adsorption of BH^{4-} ions and electrophilic dye molecules on the AuNPs affects its standard electrode potentials, allowing quicker electron transport, in which the AuNPs may serve as a redox center, transporting electrons from the BH^{4-} to the dye substrate. Fig. 14 represents the scheme proposed for the AuNPs mediated catalytic the reduction of dyes.

Table 2 compares the catalytic activity of the prepared AuNPs to that of metal-based catalytic systems reported earlier.

The study demonstrates that clammy cherry stabilized

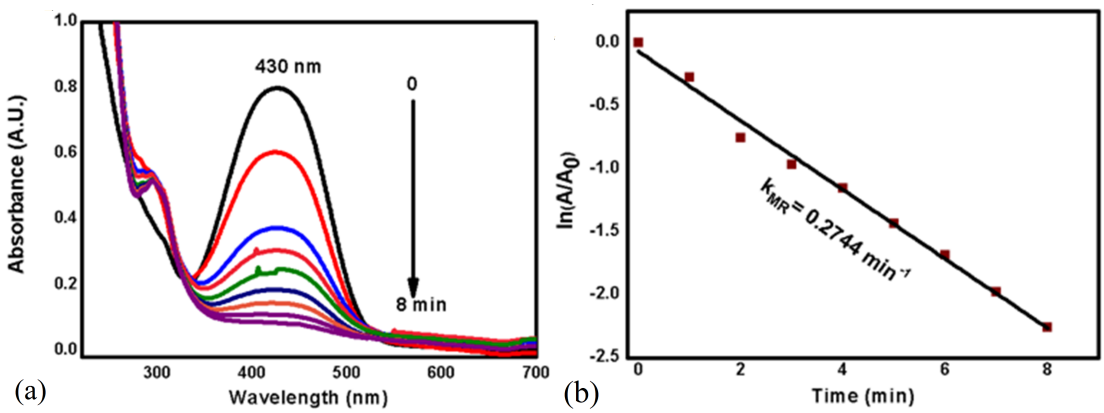

Figure 11. UV-Visible absorption spectra for the AuNPs catalyzed reduction of MR (a) and plot of ln (A/A_0) against time (b).

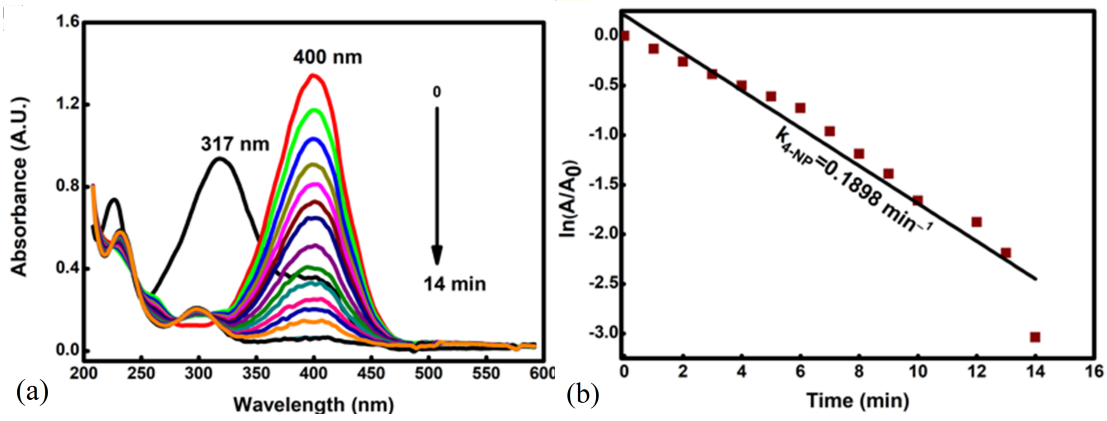

Figure 12. UV-Visible absorption spectra for the AuNPs catalyzed reduction of 4-NP (a) and plot of ln (A/A_0) against time (b).

AuNPs have comparable catalytic effectiveness for reductive discoloration of a wide variety of organic substrates. The improved stability and compact size of the produced AuNPs are related to the high catalytic activity. As a result of the study, it was proven that the cherry-protected stable AuNPs-based catalytic devices can be effectively employed to eliminate hazardous organic pollutants.

3.6 Anticancer activity of AuNPs

The anticancer property of biosynthesized AuNP colloid was investigaed with DLA cells, the result of the study is given in Table 3. Figures 15 (A, B, C, D, E) respectively represents the morphological changes AuNPs on DLA cells. The data showed that AuNPs colloid could reduce the viability of DLA cells in a dose dependant manner and it is significant that the colloid as such where the active AuNPs concentration was much lower could show considerable biological potency. This may be due to the reactive oxygen species induced by nanoparticles, it causes damages to the cellular component and leads to the cell death [61]. The quantification of anticancer activity was estimated and represented as bar diagram in Fig. 15 (F).

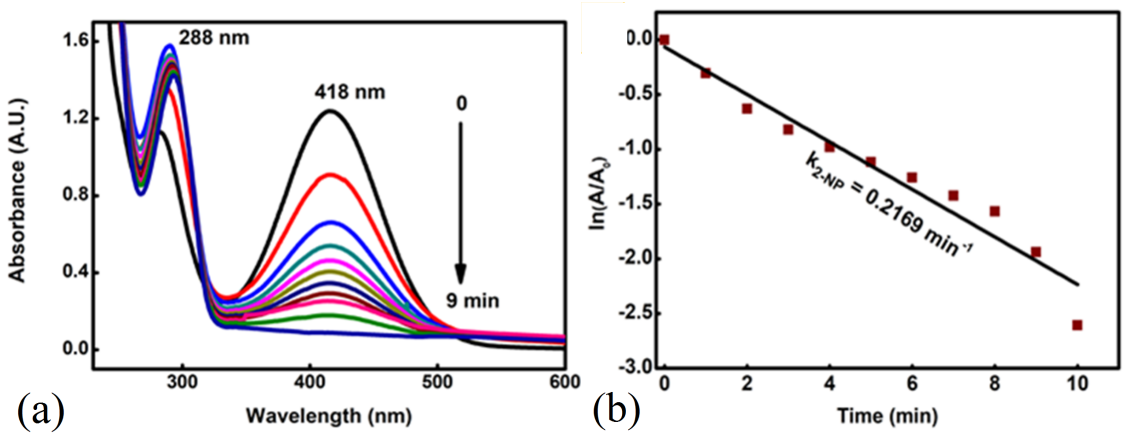

Figure 13. UV-Visible absorption spectra for the reduction of 2-NP catalyzed by AuNPs (a) and plot of ln(A/A_0) against time (b).

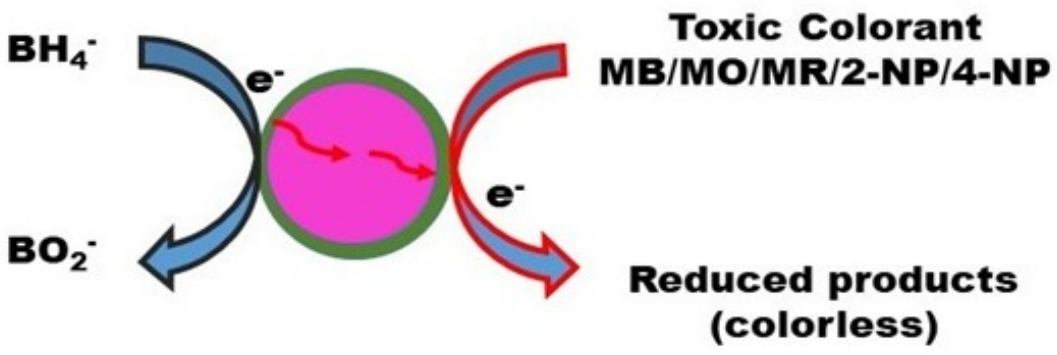

Figure 14. A proposed scheme for reduction of dye by $NaBH_4$ in the presence of AuNPs.

Table 2. Comparison of catalytic activity of the synthesized AuNPs with some reported works.

System	Substrate	Rate constant (min^{-1})	Reference
AgNPs-PVA	MB	0.0218	[50]
AuNPs	MB	0.241	[51]
AuNPs	2-NP	0.17	[52]
Ag –Zeolite X	MO	0.305	[53]
AgNPs	MO	0.0186	[54]
PdAu/Dens-OH	MO	0.0948	[55]
AgNPs	MO	0.3038	[46]
AuNPs	4-NP	0.026	[56]
PdNPs	4-NP	0.11	[57]
AgNPs	MB	0.2173	[41]
PdNPs	4-NP	0.183	[58]
AuNPs	**MO**	**0.6730**	
AuNPs	**4-NP**	**0.1898**	
AuNPs	**MB**	**0.5014**	This work
AuNPs	**2-NP**	**0.2169**	
AuNPs	**MR**	**0.2744**	

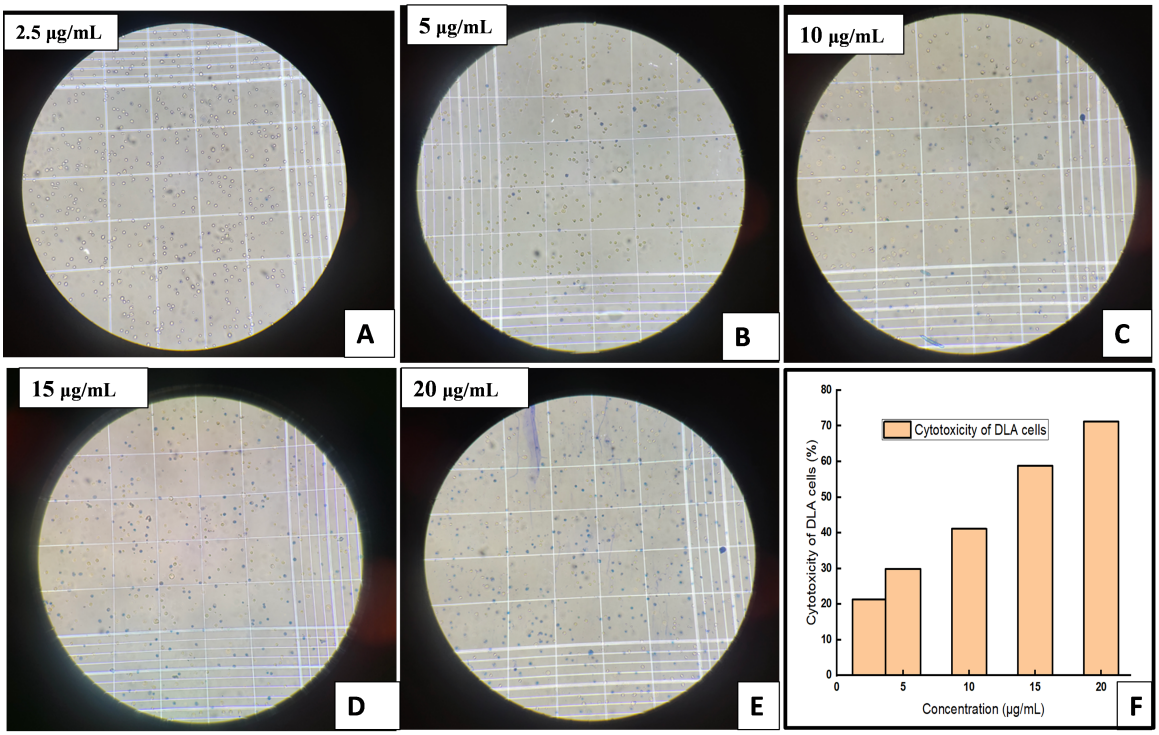

Figure 15. Analysis of *in vitro* cancer cell cytotoxicity of AuNPs (A–E). The quantification of anticancer activity was estimated and represented as bar diagram (F).

Table 3. Anticancer activity of AuNPs against DLA cells.

Concentration (μg/mL)	% Cell Death
	DLA cells
2.5	21.3±1.6
5	29.9±1.9
10	41.1±3.1
15	58.8±1.6
20	71.2±1.8

4. Conclusion

This study presents a rapid, cost-effective, and eco-friendly approach for synthesizing gold nanoparticles (AuNPs) using clammy cherry extract under microwave irradiation. The successful reduction of Au^{3+} ions and the formation of AuNPs with an average size of 11.7 nm and a narrow size distribution highlight the efficiency of polyfunctional biomolecules in the extract, acting as both reducing and stabilizing agents. Comprehensive characterization using FTIR, UV-Vis, SEM, and TEM confirmed the structural and morphological properties of the synthesized AuNPs. The biosynthesized AuNPs demonstrated significant anticancer activity against DLA cells, indicating their potential biomedical applications. Additionally, their effectiveness as heterogeneous catalysts in the reductive degradation of dyes and nitro compounds suggests their applicability in waste water treatment for the removal of toxic pollutants. Further research is ongoing to explore their electrochemical behaviour and antibacterial properties, expanding their potential in various scientific and industrial domains.

Authors contributions
Authors have contributed equally in preparing and writing the manuscript.

Availability of data and materials
The authors declare that the data supporting the findings of this study are available within the paper.

Conflict of interests
The authors assert that they do not have any identifiable conflicting financial interests or personal relationships that might be perceived to influence the work presented in this paper.

References

[1] A. A. Yaqoob, H. Ahmad, T. Parveen, A. Ahmad, M. Oves, I. M. Ismail, H. A. Qari, K. Umar, and M. N. M. Ibrahim. "Recent advances in metal decorated nanomaterials and their various biological applications: A review.". *Front. Chem.*, 8:341–362, 2020.
DOI: https://doi.org/10.3389/fchem.2020.00341.

[2] M. A. S. Sadjadi, M. Meskinfam, B. Sadeghi, H. Jazdarreh, and K. Zare. "In situ biomimetic synthesis and characterization of nano hydroxyapatite in gelatin matrix.". *J. Biomed. Nanotechnol.*, 7:450–454, 2011.
DOI: https://doi.org/10.1166/jbn.2011.1305.

[3] B. Sadeghi, S. Ghammamy, Z. Gholipour, M. Ghorchibeigy, and A. A. Nia. "Gold/hydroxypropyl cellulose hybrid nanocomposite constructed with more complete coverage of gold nano-shell.". *Nanomicro Lett.*, 6:4, 2011.
DOI: https://doi.org/10.1049/mnl.2011.0036.

[4] A. Amininia, K. Pourshamsian, and B. Sadeghi. "Nano-ZnO impregnated on starch—A highly efficient heterogeneous bio-based catalyst for one-pot synthesis of pyranopyrimidinone and xanthene derivatives as potential antibacterial agents.". *Russ J Org Chem.*, 56:1279–1288, 2020.
DOI: https://doi.org/10.1134/S1070428020070234.

[5] B. Sadeghy and S. Ghammami. "Oxidation of alcohols with tetramethylammonium fluorochromate in aceticoi acid.". *Russ J Gen Chem.*, 75:1886–1888, 2005.
DOI: https://doi.org/10.1007/s11176-006-0008-0.

[6] M. S. Sadjadi, B. Sadeghi, and K. Zare. "Natural bond orbital (NBO) population analysis of cyclic thionylphosphazenes, [NSOX (NPCl2)2]; X = F (1), X = Cl (2).". *J. Mol. Struct. THEOCHEM*, 817:27–33, 2007.
DOI: https://doi.org/10.1016/j.theochem.2007.04.015.

[7] H. Singh, A. Bamrah, S. K. Bhardwaj, A. Deep, M. Khatri, R. J. C. Brown, N. Bhardwaj, and K. H. Kim. "Recent advances in the application of noble metal nanoparticles in colorimetric sensors for lead ions.". *Environ Sci Nano*, 8:863–889, 2021.
DOI: https://doi.org/10.1039/D0EN00963F.

[8] V. Pareek, A. Bhargava, R. Gupta, J. Navin, and P. Jitendra. "Synthesis and applications of noble metal nanoparticles: A review.". *Adv Sci Eng Med*, 9:527–544, 2017.
DOI: https://doi.org/10.1166/asem.2017.2027.

[9] N. Assad, M. Naeem-ul Hassan, M. A. Hussain, A. Abbas, M. Sher, G. Muhammad, Y. Assad, and M. Farid-ul Haq. "Diffused sunlight assisted green synthesis of silver nanoparticles using Cotoneaster nummularia polar extract for antimicrobial and wound healing applications.". *Nat. Prod. Res.*, pages 1–15, 2023.
DOI: https://doi.org/10.1080/14786419.2023.2295936.

[10] S. Ullah, R. Khalid, M. F. Rehman, M. I. Irfan, A. Abbas, A. Alhoshani, F. Anwar, and H. M. A. Amin. "Biosynthesis of phytofunctionalized silver nanoparticles using olive fruit extract and evaluation of their antibacterial and antioxidant properties.". *Front. Chem.*, 11:1202252, 2023.
DOI: https://doi.org/10.3389/fchem.2023.1202252.

[11] S. M. Ghoreishi and S. M. Derazkola. "Eco-friendly synthesis of gold nanoparticles via tangerine peel extract: Unveiling their multifaceted biological and catalytic potentials.". *Heliyon*, 11(1), 2025.
DOI: https://doi.org/10.1016/j.heliyon.2024.e40104.

[12] M. Zare-Bidaki, H. Aramjoo, Z. M. Mizwari, P. M. Tabas, R. Javanshir, and S. Mortazavi-Derazkola. "Cytotoxicity, antifungal, antioxidant, antibacterial and photodegradation potential of silver nanoparticles mediated via Medicago sativa extract.". *Arab. J. Chem.*, 15:103842, 2022.
DOI: https://doi.org/10.1016/j.arabjc.2022.103842.

[13] M. S. Ahodashti, Hashemi, Y. Mortazavi, K. Khormali, S. Mortazavi-Derazkola, and M. A. Ebrahimzadeh. "Discovery of high antibacterial and catalytic activities against multi-drug resistant clinical bacteria and hazardous pollutants by biosynthesized of silver nanoparticles using Stachys inflata extract (AgNPs@SI).". *Colloids Surf. A: Physicochem.*, 617:126383, 2021.
DOI: https://doi.org/10.1016/j.colsurfa.2021.126383.

[14] Z. Hashemi, Z. M. Mizwari, S. R. Alizadeh, M. Habibi, S. Mohammadrezaee, S. M. Ghoreishi, S. Mortazavi-Derazkola, and M. A. Ebrahimzadeh. "Anticancer and antibacterial activity against clinical pathogenic multi-drug resistant bacteria using biosynthesized silver nanoparticles with Mentha pulegium and Crocus caspius extracts.". *Inorg. Chem. Commun.*, 154:110982, 2023.
DOI: https://doi.org/10.1016/j.inoche.2023.110982.

[15] M. Shirzadi-Ahodashti, Z. M. Mizwaric, S. Mohammadi-Aghdam, S. Ahmadi, M. A. Ebrahimzadeh, and S. Mortazavi-Derazkola. "Optimization and evaluation of anticancer, antifungal, catalytic, and antibacterial activities: Biosynthesis of spherical-shaped gold nanoparticles using Pistacia vera hull extract (AuNPs@PV).". *Arab. J. Chem.*, 16(1):104423, 2023.
DOI: https://doi.org/10.1016/j.arabjc.2022.104423.

[16] Z. Hashemi, Z. M. Mizwari, Z. Hosseini, Z. Khosravi, S. R. Alizadeh, M. Shirzadi-Ahodashti, A. Asadipour, S. M. Ghoreishi, M. A. Ebrahimzadeh, and S. Mortazavi-Derazkola. "In-vitro anticancer and antibacterial activities and comparative of eco-friendly synthesized silver nanoparticles using hull of Pistacia vera and rhizome of Sambucus ebulus extracts.". *Inorg. Chem. Commun.*, 154:110913, 2023.
DOI: https://doi.org/10.1016/j.inoche.2023.110913.

[17] F. Barzegarparay, H. Najafzadehvarzi, R. Pourbagher, H. Parsian, S. A. Ghoreishi, and S. Mortazavi-Derazkola. "Green synthesis of novel selenium nanoparticles using Crataegus monogyna extract (SeNPs@CM) and investigation of its toxicity, antioxidant capacity, and anticancer activity against MCF-7 as a breast cancer cell line.". *Biomass Conv. Bioref.*, 14:25369–25378, 2024.
DOI: https://doi.org/10.1007/s13399-023-04604-z.

[18] Z. Kiani, H. Aramjoo, E. Chamani, M. Siami-Aliabad, and S. Mortazavi-Derazkola. "In vitro cytotoxicity against K562 tumor cell line, antibacterial, antioxidant, antifungal and catalytic activities of biosynthesized silver nanoparticles using Sophora pachycarpa extract.". *Arab. J. Chem.*, 3:103677, 2022.
DOI: https://doi.org/10.1016/j.arabjc.2021.103677.

[19] S. Mohammadi-Aghdam, F. Bahraini, and S. M. Ghoreishi. "In-vitro anticancer on acute lymphoblastic leukemia NALM-6 cell line, antibacterial and catalytic performance of eco-friendly synthesized ZnO and Ag-doped ZnO nanoparticles using Hedera colchica extract.". *Biomass Convers Biorefin.*, 14:1–16, 2023.
DOI: https://doi.org/10.1007/s13399-023-04562-6.

[20] S. A. Bansal, V. Kumar, J. Karimi, A. P. Singh, and S. Kumar. "Role of gold nanoparticles in advanced biomedical applications.". *Nanoscale Adv*, 2:3764–3787, 2020.
DOI: https://doi.org/10.1039/D0NA00472C.

[21] P. Chhour, P. C. Naha, R. Cheheltani, B. Benardo, S. Mian, and D. P. Cormode. "Gold nanoparticles for biomedical applications: Synthesis and in vitro evaluation.". *Nanomaterials in Pharmacology*, pages 87–111, 2016.

[22] A. Shah, S. Akhtar, F. Mahmood, S. Urooj, A. B. Siddique, M. I. Irfan, M. N. Hassan, M. Sher, A. Alhoshani, A. Rauf, H. M. A. Amin, and A. Abbas. "Fagonia arabica extract-stabilized gold nanoparticles as a highly selective colorimetric nanoprobe for Cd2+ detection and as a potential photocatalytic and antibacterial agent.". *Surf. Interfaces*, 51:104556, 2024.
DOI: https://doi.org/10.1016/j.surfin.2024.104556.

[23] A. W. Khan, N. S. Lali, F. Y. Sabei, M. I. Irfan, M. N. Hassan, M. Sher, A. Y. Safhi, A. Alsalhi, A. H. Albariqi, F. Kamli, H. M. A. Amin, and A. Abbas. "Sunlight-assisted green synthesis of gold nanocubes using horsetail leaf extract: A highly selective colorimetric sensor for Pb2+, photocatalytic and antimicrobial agent.". *J. Environ. Chem. Eng.*, 12:112576, 2024.
DOI: https://doi.org/10.1016/j.jece.2024.112576.

[24] A. Ejaz, Z. Mamtaz, I. Yasmin, M. Shaban, A. B. Siddique, M. I. Irfan, A. Ali, S. Muhammad, M. Y. Sameeh, and A. Abbas. "Cyperus scariosus extract based greenly synthesized gold nanoparticles as colorimetric nanoprobe for Ni2+ detection and as antibacterial and photocatalytic agent.". *J. Mol. Liq.*, 393:123622, 2024.
DOI: https://doi.org/10.1016/j.molliq.2023.123622.

[25] A. Jabbar, A. Abbas, N. Assad, M. N. Hassan, H. A. Alhazmi, A. Najmi, K. Zoghebi, A. I. Bratty, A. Hanbashi, and H. M. A. Amin. "A highly selective Hg2+ colorimetric sensor and antimicrobial agent based on green synthesized silver nanoparticles using Equisetum diffusum extract.". *RSC Adv.*, 13:28666–28675, 2023.
DOI: https://doi.org/10.1039/D3RA05070J.

[26] A. B. Siddique, D. Amr, A. Abbas, L. Zohra, M. I. Irfan, A. Alhoshani, S. Ashraf, and H. M. A. Amin. "Synthesis of hydroxyethylcellulose phthalate-modified silver nanoparticles and their multifunctional applications as an efficient antibacterial, photocatalytic and mercury-selective sensing agent.". *Int. J. Biol. Macromol.*, 256: 128009, 2024.
DOI: https://doi.org/10.1016/j.ijbiomac.2023.128009.

[27] S. Amin, M. Sher, A. Ali, M. F. Rehman, A. Hayat, M. Ikram, A. Abbas, and H. M. A. Amin. "Sulfonamide-functionalized silver nanoparticles as an analytical nanoprobe for selective Ni(II) sensing with synergistic antimicrobial activity.". *Environ. Nanotechnol. Monit. Manag.*, 18:100735, 2022.
DOI: https://doi.org/10.1016/j.enmm.2022.100735.

[28] S. Chaturvedi, P. N. Dave, and N. K. Shah. "Applications of nano-catalyst in new era.". *J Saudi Chem Soc*, 16:307–325, 2022.
DOI: https://doi.org/10.1016/j.jscs.2011.01.015.

[29] Z. U. H. Khan, A. Khan, Y. Chen, A. Khan, N. S. Shah, N. Muhammad, B. Murtaza, K. Tahir, F. U. Khan, and P. Wan. "Photo catalytic applications of gold nanoparticles synthesized by green route and electrochemical degradation of phenolic Azo dyes using AuNPs /GC as modified paste electrode.". *J Alloys Compd*, 725, 2017.
DOI: https://doi.org/10.1016/j.jallcom.2017.07.222.

[30] G. J. Hutchings and J. K. Edwards. "Chapter 6 - Application of gold nanoparticles in catalysis.". *Metal Nanoparticles and Nanoalloys*, pages 249–293, 2012.

[31] Y. C. Chang and D. H. Chen. "Catalytic reduction of 4-nitrophenol by magnetically recoverable Au nanocatalyst.". *J Hazard Mater*, 165:664–669, 2009.
DOI: https://doi.org/10.1016/j.jhazmat.2008.10.034.

[32] G. Sharma, A. Kumar, S. Sharma, M. Naushad, R. P. Dwivedi, Z. A. AlOthman, and G. T. Mola. "Novel development of nanoparticles to bimetallic nanoparticles and their composites: A review.". *J King Saud Univ - Sci*, 31:257–269, 2019.
DOI: https://doi.org/10.1016/j.jksus.2017.06.012.

[33] S. Francis, E. P. Koshy, and B. Mathew. "Microwave aided synthesis of silver and gold nanoparticles and their antioxidant , antimicrobial and catalytic potentials.". *J Nanostruct*, 8:55–66, 2018.
DOI: https://doi.org/10.22052/JNS.2018.01.007.

[34] K. H. Huynh, X. H. Pham, J. Kim, S. H. Lee, H. Chang, W. Y. Rho, and B. H. Jun. "Synthesis, properties, and biological applications of metallic alloy nanoparticles.". *Int J Mol Sci*, 21:1–29, 2020.
DOI: https://doi.org/10.3390/ijms21145174.

[35] P. Dauthal and M. Mukhopadhyay. "Noble metal nanoparticles: Plant-mediated synthesis, mechanistic aspects of synthesis, and applications.". *Ind Eng Chem Res*, 55:9557–9577, 2016.
DOI: https://doi.org/10.1021/acs.iecr.6b00861.

[36] C. E. A. Botteon, L. B. Silva, G. V. Ccana-Ccapatinta, T. S. Silva, S. R. Ambrosio, R. C. S. Veneziani, J. K. Bastos, and P. D. Marcato. "Biosynthesis and characterization of gold nanoparticles using Brazilian red propolis and evaluation of its antimicrobial and anticancer activities.". *Sci Rep*, 11:1974, 2021.
DOI: https://doi.org/10.1038/s41598-021-81281-w.

[37] J. Santhoshkumar, S. Rajeshkumar, and S. Venkat Kumar. "Phyto-assisted synthesis, characterization and applications of gold nanoparticles – A review.". *Biochem Biophys Reports*, 11:46–57, 2017.
DOI: https://doi.org/10.1016/j.bbrep.2017.06.004.

[38] A. Gudie Assefa, A. Adugna Mesfin, M. Legesse Akele, M. Kokeb Alemu, V. Reddy Ganapuram, V. Guttena, and M. Alle. "Microwave-assisted green synthesis of gold nanoparticles using olibanum gum (boswellia serrate) and its catalytic reduction of 4-nitrophenol and hexacyanoferrate (III) by sodium borohydride.". *J Clust Sci.*, 2017.
DOI: https://doi.org/10.1007/s10876-016-1078-8.

[39] B. I. Kharisov, O. V. Kharissova, and U. O. Méndez. "Microwave hydrothermal and solvothermal processing of materials and compounds.". 2012.

[40] U. Riaz, S. M. Ashraf, S. Aleem, V. Budhiraja, and S. Jadoun. "Microwave-assisted green synthesis of some nanoconjugated copolymers: characterisation serum albumin.". *New J Chem*, 40:4643–4653, 2016.
DOI: https://doi.org/10.1039/c5nj02513c.

[41] S. Francis, S. Joseph, E. P. Koshy, and B. Mathew. "Microwave assisted green synthesis of silver nanoparticles using leaf extract of elephantopus scaber and its environmental and biological applications.". *Artif Cells, Nanomedicine Biotechnol*, 46:795–804, 2018.
DOI: https://doi.org/10.1080/21691401.2017.1345921.

[42] K. C. Hsu and D. H. Chen. "Microwave-assisted green synthesis of Ag/reduced graphene oxide nanocomposite as a surface-enhanced Raman scattering substrate with high uniformity.". *Nanoscale Res Lett*, 9:1–9, 2014.
DOI: https://doi.org/10.1186/1556-276X-9-193.

[43] M. J. Oza and Y. A. Kulkarni. "Traditional uses, phytochemistry and pharmacology of the medicinal species of the genus Cordia (Boraginaceae).". *J Pharm Pharmacol*, 69:755–789, 2017.
DOI: https://doi.org/10.1111/jphp.12715.

[44] R. Gupta and G. Das Gupta. "Isolation and characterization of flavonoid glycoside from Cordia obliqua Willd. leaf.". *Int J Green Pharm*, 17:73–79, 2018.

[45] J. S. Chauhan, S. K. Srivastava, and M. Sultan. "Hesperetin 7-rhamnoside from Cordia obliqua.". *Phytochemistry*, 17:334, 1978.
DOI: https://doi.org/10.1016/S0031-9422(00)94187-6.

[46] F. K. Saidu, A. Mathew, A. Parveen, V. Valiyathra, and G. V. Thomas. "Novel green synthesis of silver nanoparticles using clammy cherry (Cordia obliqua Willd) fruit extract and investigation on its catalytic and antimicrobial properties.". *SN Appl Sci*, 1:1368–1380, 2019.
DOI: https://doi.org/10.1007/s42452-019-1302-x.

[47] V. Amendola. "Surface plasmon resonance of silver and gold nanoparticles in the proximity of graphene studied using the discrete dipole approximation method.". *Phys Chem Chem Phys*, 18: 2230–2241, 2016.
DOI: https://doi.org/10.1039/C5CP06121K.

[48] V. Amendola, R. Pilot, M. Frasconi, O. M. Marago, and M. Antonia lati. "Surface plasmon resonance in gold nanoparticles: A review.". *J Phys Condens Matter*, 29:203002, 2017.
DOI: https://doi.org/10.1088/1361-648x/aa60f3.

[49] X. Huang and M. A. El-Sayed. "Gold nanoparticles: Optical properties and implementations in cancer diagnosis and photothermal therapy.". *J Adv Res*, 1:13–28, 2010.
DOI: https://doi.org/10.1016/j.jare.2010.02.002.

[50] P. Sagitha, K. Sarada, and K. Muraleedharan. "One-pot synthesis of poly vinyl alcohol (PVA) supported silver nanoparticles and its efficiency in catalytic reduction of methylene blue.". *Trans Nonferrous Met Soc China (English Ed)*, 26:2693–2700, 2016.
DOI: https://doi.org/10.1016/S1003-6326(16)64397-2.

[51] B. R. Ganapuram, M. Alle, R. Dadigala, A. Dasari, V. Maragoni, and V. Guttena. "Catalytic reduction of methylene blue and Congo red dyes using green synthesized gold nanoparticles capped by salmalia malabarica gum.". *Int Nano Lett*, 5:215–222, 2015.
DOI: https://doi.org/10.1007/s40089-015-0158-3.

[52] H. Liu and Q. Yang. "Facile fabrication of nanoporous Au-Pd bimetallic foams with high catalytic activity for 2-nitrophenol reduction and SERS property.". *J Mater Chem*, 11:11961–11967, 2011.
DOI: https://doi.org/10.1039/c1jm10109a.

[53] A. Zainal Abidin, N. H. H. Abu Bakar, E. P. Ng, and W. L. Tan. "Rapid degradation of methyl orange by Ag doped zeolite X in the presence of borohydride.". *J Taibah Univ Sci*, 11:1070–1079, 2017.
DOI: https://doi.org/10.1016/j.jtusci.2017.06.004.

[54] K. Jyoti and A. Singh. "Green synthesis of nanostructured silver particles and their catalytic application in dye degradation.". *J Genet Eng Biotechnol*, 14:311–317, 2016.
DOI: https://doi.org/10.1016/j.jgeb.2016.09.005.

[55] A. K. Ilunga, T. Khoza, E. Tjabadi, and R. Meijboom. "Effective catalytic reduction of methyl orange catalyzed by the encapsulated random alloy palladium-gold nanoparticles dendrimer.". *ChemistrySelect*, 2:9803–9809, 2017.
DOI: https://doi.org/10.1002/slct.201701631.

[56] K. B. Narayanan, H. H. Park, and N. Sakthivel. "Extracellular synthesis of mycogenic silver nanoparticles by Cylindrocladium floridanum and its homogeneous catalytic degradation of 4-nitrophenol.". *Spectrochim Acta Part A Mol Biomol Spectrosc*, 116:485–490, 2013.
DOI: https://doi.org/10.1016/j.saa.2013.07.066.

[57] A. J. Kora and L. Rastogi. "Green synthesis of palladium nanoparticles using gum ghatti (Anogeissus latifolia) and its application as an antioxidant and catalyst.". *Arab J Chem*, 11:1097–1106, 2018.
DOI: https://doi.org/10.1016/j.arabjc.2015.06.024.

[58] M. Sathishkumar, K. Sneha, I. S. Kwak, Juan Mao, and S. J. Tripathy. "Phyto-crystallization of palladium through reduction process using Cinnamom zeylanicum bark extract.". *J Hazard Mater*, 171:400–404, 2009.
DOI: https://doi.org/10.1016/j.jhazmat.2009.06.014.

[59] A. Murugadoss and A. Chattopadhyay. "A "green" chitosan-silver nanoparticle composite as a heterogeneous as well as micro-heterogeneous catalyst.". *Nanotechnology*, 19, 2008.
DOI: https://doi.org/10.1088/0957-4484/19/01/015603.

[60] A. Omidvar, B. Jaleh, and M. Nasrollahzadeh. "Preparation of the GO/Pd nanocomposite and its application for the degradation of organic dyes in water.". *J Colloid Interface Sci*, 496:44–50, 2017.
DOI: https://doi.org/10.1016/j.jcis.2017.01.113.

[61] S. J. Packia Jacob, J. S. Finub, and A. Narayanan. "Synthesis of silver nanoparticles using Piper longum leaf extracts and its cytotoxic activity against Hep-2 cell line.". *Colloids Surf B Biointerfaces*, 9: 212–214, 2012.